



This is a repository copy of *Evolution of size-dependent flowering in a variable environment: construction and analysis of a stochastic integral projection model* .

White Rose Research Online URL for this paper:
<http://eprints.whiterose.ac.uk/1396/>

Article:

Childs, D.Z., Rees, M., Rose, K.E. et al. (2 more authors) (2004) Evolution of size-dependent flowering in a variable environment: construction and analysis of a stochastic integral projection model. *Proceedings of the Royal Society B: Biological Sciences*, 271 (1537). pp. 425-434. ISSN 1471-2954

<https://doi.org/10.1098/rspb.2003.2597>

Reuse

Unless indicated otherwise, fulltext items are protected by copyright with all rights reserved. The copyright exception in section 29 of the Copyright, Designs and Patents Act 1988 allows the making of a single copy solely for the purpose of non-commercial research or private study within the limits of fair dealing. The publisher or other rights-holder may allow further reproduction and re-use of this version - refer to the White Rose Research Online record for this item. Where records identify the publisher as the copyright holder, users can verify any specific terms of use on the publisher's website.

Takedown

If you consider content in White Rose Research Online to be in breach of UK law, please notify us by emailing eprints@whiterose.ac.uk including the URL of the record and the reason for the withdrawal request.



eprints@whiterose.ac.uk
<https://eprints.whiterose.ac.uk/>

Evolution of size-dependent flowering in a variable environment: construction and analysis of a stochastic integral projection model

Dylan Z. Childs¹, Mark Rees^{1*}, Karen E. Rose¹, Peter J. Grubb²
and Stephen P. Ellner³

¹Department of Biological Sciences and NERC Centre for Population Biology, Imperial College, Silwood Park, Ascot SL5 7PY, UK

²Department of Plant Sciences, University of Cambridge, Cambridge CB2 3EA, UK

³Department of Ecology and Evolutionary Biology, Corson Hall, Cornell University, Ithaca, NY 14853-2701, USA

Understanding why individuals delay reproduction is a classic problem in evolutionary biology. In plants, the study of reproductive delays is complicated because growth and survival can be size and age dependent, individuals of the same size can grow by different amounts and there is temporal variation in the environment. We extend the recently developed integral projection approach to include size- and age-dependent demography and temporal variation. The technique is then applied to a long-term individually structured dataset for *Carlina vulgaris*, a monocarpic thistle. The parameterized model has excellent descriptive properties in terms of both the population size and the distributions of sizes within each age class. In *Carlina*, the probability of flowering depends on both plant size and age. We use the parameterized model to predict this relationship, using the evolutionarily stable strategy approach. Considering each year separately, we show that both the direction and the magnitude of selection on the flowering strategy vary from year to year. Provided the flowering strategy is constrained, so it cannot be a step function, the model accurately predicts the average size at flowering. Elasticity analysis is used to partition the size- and age-specific contributions to the stochastic growth rate, λ_s . We use λ_s to construct fitness landscapes and show how different forms of stochasticity influence its topography. We prove the existence of a unique stochastic growth rate, λ_s , which is independent of the initial population vector, and show that Tuljapurkar's perturbation analysis for $\log(\lambda_s)$ can be used to calculate elasticities.

Keywords: fluctuating selection; fitness landscape; stochastic growth rate; evolutionarily stable strategy

1. INTRODUCTION

Natural systems are often highly variable, yet the majority of life-history studies assume a constant density-independent environment (reviews in Roff 1992 and Stearns 1992). These assumptions allow fitness to be assessed in terms of simple measures of population growth rate such as r , the intrinsic rate of increase, or R_0 , the net reproductive rate (Charlesworth 1994). However, this approach is appropriate only in a constant environment, where population growth is unconstrained or particular forms of density dependence operate (Mylius & Diekmann 1995). When there is environmental stochasticity or a non-equilibrium attractor, theory predicts that the fitness of a given life-history strategy may be quite different (Tuljapurkar 1990; Rand *et al.* 1994). For example, in a density-regulated population the fitness of a strategy depends on the other life histories present. Under such conditions, fitness should be measured using the 'invasion exponent' ϑ , which is the logarithmic growth rate of an invading population growing in an environment defined by the resident population (Metz *et al.* 1992; Mylius & Diekmann 1995). Failure to use invasibility analysis based on ϑ may result in

imprecise or even qualitatively incorrect predictions about optimal life-history strategies.

Typically, the demography of a structured population is investigated by constructing a matrix model, where individuals are placed into discrete categories defined by age, stage or size class (Caswell 2001). However, such models are not strictly appropriate for continuously structured populations, as the choice of categories may affect the predictions of the model (Easterling *et al.* 2000). The individual-based approach provides an alternative for modelling continuously structured populations. However, though the individual-based approach is flexible, it is computationally inefficient and the underlying models are often difficult to describe. The recently developed integral projection model provides an elegant framework for projecting a continuously structured population in discrete time (Easterling *et al.* 2000; Rees & Rose 2002; Childs *et al.* 2003), yet until now this approach was limited to constant environments. We demonstrate how it is possible to extend the integral projection model to represent a stochastic density-dependent environment, and further develop the approach to include an additional discrete structuring variable such as age. Coupled with modern techniques of invasibility analysis, this approach allows detailed assessment of the role of stochasticity in shaping evolution, using simple field data.

* Author for correspondence (m.rees@imperial.ac.uk).

We use these techniques to explore why organisms defer reproduction, a classic problem in evolutionary biology (Cole 1954). The main benefits of early reproduction accrue through reductions in mortality and generation time, while the costs of early reproduction are reduced fecundity and/or quality of offspring (Cole 1954; Roff 1992; Stearns 1992). In plants, the study of reproductive delays is complicated because plants vary continuously in size and there is enormous variation in growth between individuals. Several studies have attempted to predict the optimal size of flowering in semelparous plants, using a variety of approaches. These approaches include analytical approximations, dynamic state variable models or computationally expensive individual-based models (Kachi & Hirose 1985; de Jong *et al.* 1989, 2000; Wesselingh *et al.* 1997; Rees *et al.* 1999, 2000; Rees & Rose 2002; Rose *et al.* 2002). Rees *et al.* (1999) compared these different approaches by developing a series of parameterized demographic models of the monocarpic thistle *Onopordum illyricum* and found that an accurate prediction of flowering size was possible only when using an individual-based model. More recently, Rose *et al.* (2002) were able to predict the optimal flowering size of another monocarpic thistle, *Carlina vulgaris*, using an individual-based approach. Both these studies emphasized the need to incorporate stochastic variation into life-history analyses.

We explore the evolution of size- and age-dependent flowering in the monocarpic thistle *C. vulgaris*. The probability of flowering in *Carlina*, as in several other monocarpic species, is a function of plant size and age (Klinkhamer *et al.* 1987; Rees *et al.* 1999; Rose *et al.* 2002). First, we outline the construction of stochastic integral projection models for monocarpic plants with size- and age-dependent demographic rates. We then summarize the size- and age-dependent demography of *Carlina*. Using invasibility analysis, we then test whether the estimated strategy is adaptive in a stochastic environment. We generate fitness landscapes under different stochasticity regimes to test whether they are consistent with our interpretation of the evolutionarily stable strategy (ESS) calculations. Finally, we carry out elasticity analysis as a further comparison of mutant fitness in constant and stochastic environments. We prove the existence of a unique stochastic growth rate, λ_s , which is independent of the initial population vector for the stochastic integral projection model, and show that Tuljapurkar's perturbation analysis for $\log(\lambda_s)$ can be used to calculate elasticities (Tuljapurkar 1990).

2. METHODS

(a) Stochastic integral projection models

The integral projection model can be used to describe how a continuously size-structured population changes in discrete time (Easterling *et al.* 2000). The state of the population is described by a probability density function, $n(x, t)$, which can intuitively be thought of as the proportion of individuals that are of size x at time t . The integral projection model for the proportion of individuals that are of size y at time $t + 1$, 1 year later, is then given by

$$n(y, t + 1) = \int_{\Omega} [p(x, y) + f(x, y)]n(x, t)dx = \int_{\Omega} k(y, x)n(x, t)dx, \tag{2.1}$$

where $k(y, x)$, known as the kernel, describes all possible transitions from size x to size y , including births. The integration is over the set of all possible sizes, Ω . The kernel is composed of two parts, a fecundity function, $f(x, y)$, and a survival-growth function, $p(x, y)$. To include environmental stochasticity we imagine that a model linking the environment to the demographic rates has been defined. This gives rise to a series of kernels $k^{(0)}(x, y)$, $k^{(1)}(x, y)$, ..., $k^{(t)}(x, y)$ describing the environment at each time-step until year t . The stochastic integral projection model is then given by

$$n(y, t + 1) = \int_{\Omega} k^{(t)}(x, y)n(x, t)dx. \tag{2.2}$$

To extend this basic model to include size- and age-dependent demography we define $n_a(y, t)$ to be the probability density function for individuals of size y and age a in year t (see Childs *et al.* 2003). The stochastic integral projection model then becomes

$$n_0(y, t + 1) = \sum_{a=0}^m \int_{\Omega} f_a^{(t)}(x, y)n_a(x, t)dx \quad a = 0, \tag{2.3}$$

$$n_a(y, t + 1) = \int_{\Omega} p_{a-1}^{(t)}(x, y)n_{a-1}(x, t)dx \quad a > 0,$$

where $f_a^{(t)}(x, y)$ is the fecundity function, $p_a^{(t)}(x, y)$ is the survival-growth function of plants of size x and age a in year t , and m is maximum plant age. These functions are referred to collectively as the kernel component functions. For a numerical solution, it is convenient to write the model in matrix form as

$$\mathbf{n}(y, t + 1) = \int_{\Omega} \mathbf{K}^{(t)}\mathbf{n}(x, t)dx, \tag{2.4}$$

where \mathbf{K} is the matrix

$$\mathbf{K}^{(t)} = \begin{pmatrix} f_0^{(t)}(x, y) & f_1^{(t)}(x, y) & \dots & f_{m-1}^{(t)}(x, y) & f_m^{(t)}(x, y) \\ p_0^{(t)}(x, y) & 0 & \dots & 0 & 0 \\ \vdots & p_1^{(t)}(x, y) & & \vdots & \vdots \\ & \vdots & \ddots & & \\ 0 & 0 & \dots & p_{m-1}^{(t)}(x, y) & 0 \end{pmatrix} \tag{2.5}$$

and $\mathbf{n}(y, t) = (n_0(y, t), n_1(y, t), \dots, n_m(y, t))^T$. To solve these models we use numerical integration methods (Easterling 1998). If each component function is evaluated at q evenly spaced quadrature mesh points, y_i , and w is the quadrature weight (difference between successive y_i), we can then approximate equation (2.4) as

$$\mathbf{n}(t + 1) = \tilde{\mathbf{K}}^{(t)}\mathbf{D}\mathbf{n}(t), \tag{2.6}$$

where $\mathbf{n}(t) = (n_0(y_0, t), \dots, n_0(y_q, t), \dots, n_m(y_0, t), \dots, n_m(y_q, t))^T$,

$$\tilde{\mathbf{K}}^{(t)} = \begin{pmatrix} f_0^{(t)}(y_i, y_j) & f_1^{(t)}(y_i, y_j) & \dots & f_{m-1}^{(t)}(y_i, y_j) & f_m^{(t)}(y_i, y_j) \\ p_0^{(t)}(y_i, y_j) & 0 & \dots & 0 & 0 \\ \vdots & p_1^{(t)}(y_i, y_j) & & \vdots & \vdots \\ & \vdots & \ddots & & \\ 0 & 0 & \dots & p_{m-1}^{(t)}(y_i, y_j) & 0 \end{pmatrix}, \tag{2.7}$$

and $\mathbf{D} = \text{diag}(w)$. With $\tilde{\mathbf{K}}^{(t)}$ and \mathbf{D} defined in this way, it is straightforward to iterate the stochastic integral projection model numerically by matrix multiplication,

$$\mathbf{n}(t + 1) = \tilde{\mathbf{K}}^{(t)}\mathbf{D}\tilde{\mathbf{K}}^{(t-1)}\mathbf{D} \dots \tilde{\mathbf{K}}^{(0)}\mathbf{D}\mathbf{n}(0), \tag{2.8}$$

where $\mathbf{n}(0)$ is the initial age–size vector. In all calculations, 50 evenly spaced quadrature mesh points were used. To test the accuracy of this approximation we compared the outputs of models with 50 and 200 mesh points; in all cases, there was excellent agreement.

(b) Stochastic integral projection model for *Carlina vulgaris*

To apply the model we must specify how the size and age dependences of the component functions change with time. Environments are assumed to be independent and identically distributed. Each year type, τ , is characterized by the number of recruits in the following year, $R_{\tau+1}$, and a pair of functions describing survival and growth, $s_{\tau}(x)$ and $g_{\tau}(x,y)$. These have been estimated directly from the data, giving rise to 16 function pairs for *Carlina*. For each iteration of the model, a pair of functions and the corresponding number of recruits are drawn at random from the 16 possible sets with equal probability. We write the fecundity function in year t as

$$f_a^{(t)}(x,y) = p_e(t)s_{\tau}(x)p_{f,a}(x)f_n(x)f_d(x,y), \tag{2.9}$$

where $p_e(t)$ is the probability of seedling establishment, $s_{\tau}(x)$ is the probability of survival for an individual of size x , $p_{f,a}(x)$ is the probability that an individual of size x and age a flowers, $f_n(x)$ is the number of seeds produced and $f_d(x,y)$ is the probability distribution of offspring size, y , for an individual of size x . The survival–growth function in year t is given by

$$p_a^{(t)}(x,y) = s_{\tau}(x)[1 - p_{f,a}(x)]g_{\tau}(x,y), \tag{2.10}$$

where $g_{\tau}(x,y)$ is the probability of an individual of size x growing to size y . The probability of flowering, $p_{f,a}(x)$, enters the survival–growth function, as reproduction is fatal in monocarpic species.

(c) Population biology of *C. vulgaris*

Carlina vulgaris, a monocarpic thistle of base-rich soils (mainly on limestone or calcareous sand), is found as a native over a wide area in Western, Central and Eastern Europe, and has been introduced to North America and New Zealand. Under very favourable growing conditions, *Carlina* individuals can flower in their second year (Klinkhamer *et al.* 1991, 1996; Rees *et al.* 2000) but, more commonly, reproduction is delayed by at least one more year. Previous studies in Holland (Klinkhamer *et al.* 1991, 1996) have shown that the probability of flowering is related to plant size and not to age; however, in the UK the probability of flowering is related to both plant size and age (Rose *et al.* 2002). Flowering occurs between June and August, and the seeds are retained in the flower heads until they are dispersed during dry sunny days in late autumn, winter or spring (P. J. Grubb, unpublished data). Seeds germinate from April to June, and there is little evidence of a persistent seed bank (Eriksson & Eriksson 1997; de Jong *et al.* 2000).

A detailed description of the study site and methods of analysis is given in Rose *et al.* (2002). Here, we briefly describe the main results that are relevant to this article. The study spanned 16 years and, during this time, the fates of over 1400 individuals were followed. The length of the longest leaf was used as a

measure of plant size and, in all analyses, this was transformed using natural logarithms. Growth was strongly size dependent and well described by a simple linear model

$$y = a_g + \alpha_{\tau} + b_g x + \varepsilon, \tag{2.11}$$

where α_{τ} is the deviation from the mean intercept in year type τ , and ε is a standard normal deviate with mean zero and standard deviation σ . Size this year was the most important predictor of size next year ($F_{1,492} = 919.80$, $p < 0.001$), followed by year effects ($F_{15,492} = 13.74$, $p < 0.001$). There was no significant effect of age ($F_{1,492} = 0.45$, $p = 0.501$). Therefore, the growth function $g_{\tau}(x,y)$ in a year of type τ is given by

$$g_{\tau}(x,y) = \frac{1}{\sigma\sqrt{2\pi}} \exp\left(-\frac{(y - (a_g + \alpha_{\tau} + b_g x))^2}{2\sigma^2}\right), \tag{2.12}$$

which is the normal probability density function with mean given by equation (2.11) and variance σ^2 .

Generalized linear models of the probabilities of mortality and flowering were constructed assuming binomial errors and a logit-link function. The probability of death was influenced by plant size ($\chi^2_1 = 18.6$, $p < 0.001$) but not by age ($\chi^2_1 = 2.31$, $p > 0.13$). There was significant yearly variation in mortality ($\chi^2_1 = 211.27$, $p < 0.001$) but no evidence for year–size interactions. Therefore, the survival function $s_{\tau}(x)$ in a year of type τ is described by

$$s_{\tau}(x) = \frac{\exp(m_0 + \gamma_{\tau} + m_s x)}{1 + \exp(m_0 + \gamma_{\tau} + m_s x)}, \tag{2.13}$$

where γ_{τ} is the deviation from the mean intercept of the linear predictor in a year of type τ . Plant size was the most important predictor of flowering ($\chi^2_1 = 139.86$, $p < 0.0001$), with larger plants being more likely to flower than smaller ones. There was an additional effect of age ($\chi^2_1 = 19.37$, $p < 0.001$) such that older plants were more likely to flower. The resultant flowering function $p_{f,a}(x)$ is given by

$$p_{f,a}(x) = \frac{\exp(\beta_0 + \beta_s x + \beta_a a)}{1 + \exp(\beta_0 + \beta_s x + \beta_a a)}, \tag{2.14}$$

where β_0 is the intercept, β_s the size-dependent slope and β_a the age-dependent slope of the flowering function.

There was no relationship between this year’s seed production and the number of recruits in the following year, suggesting that the probability of recruitment was density dependent (Rose *et al.* 2002). This decoupling of recruitment from seed production is probably the result of establishment being limited by the number of available microsites: more seedlings recruited when the turf was either short or opened up locally by trampling cattle (P. J. Grubb, personal observation). Thus, the probability of establishment at time t is given by

$$p_e(t) = \frac{R_{\tau+1}}{\sum_{a=0}^m \int_{\Omega} \int_{\Omega} f_{a,\tau}(x,y)n_a(x,t)dx dy}, \tag{2.15}$$

where $R_{\tau+1}$ is the number of recruits into the population following a year of type τ . Data were not available on the sizes of recruits derived from plants of different sizes, but evidence from other systems suggests a low maternal effect on recruit size (Weiner *et al.* 1997; Sletvold 2002), and so the distribution of offspring sizes was assumed to be independent of parental size. Parameter values are given in Rose *et al.* (2002).

(d) Invasibility analysis and the ESS flowering strategy

In a variable environment, fitness is determined by the invasion exponent (the dominant Lyapunov exponent), ϑ , defined by

$$\vartheta = \lim_{t \rightarrow \infty} t^{-1} E[\ln(N_t)], \quad (2.16)$$

where N_t is the total population size at time t (Tuljapurkar 1990). The number ϑ is equal to the stochastic growth rate of an invading mutant population in the environment set by the resident population, i.e. $\vartheta = \log \lambda_s$; if ϑ is negative the invader will become extinct. In Appendix A, we prove the existence of a unique stochastic growth rate that is independent of the initial population vector for the stochastic integral projection model (equation (2.3)). To estimate ϑ we assume that the invader is rare and so its density has no effect on the population growth rate. We then generate a time-series (5000 years) for the resident population consisting of the year type ($\tau_1, \tau_2, \dots, \tau_{5000}$), and the probability of establishment ($p_e^R(1), p_e^R(2), \dots, p_e^R(5000)$). This defines the environment in which we estimate ϑ . We calculate ϑ by iterating the model for the invader, using the resident time-series for τ and replacing $p_e(t)$ in equation (2.9) by $p_e^R(t)$. The maximum-likelihood estimator of the invader growth rate, $\hat{\vartheta}$, is then given by

$$\hat{\vartheta} = \frac{\ln(N_t) - \ln(N_1)}{t - 1}, \quad (2.17)$$

where N_t is the total population size at time t , that is

$$N_t = \sum_{a=0}^m \int_{\Omega} n_a(x, t) dx. \quad (2.18)$$

We can use equation (2.17) to generate a fitness landscape describing the growth rates of mutant strategies invading a given resident population. Landscapes were generated by estimating $\lambda_s (= e^{\vartheta})$ on a fixed grid of values of the flowering parameters.

To calculate the ESS we need to find a strategy that cannot be invaded by rare mutants. It can be shown that, when density dependence acts at the recruitment stage and there is no temporal variation in the environment, the ESS flowering strategy maximizes the net reproductive rate, R_0 (Mylius & Diekmann 1995). There is no theoretical justification for the use of such an optimization approach in density-dependent stochastic environments, and instead an iterative invasion process is required. We start the invasion process using the estimated flowering parameters (β_0, β_s and β_a) to generate a resident time-series, and then maximize the invasion exponent (ϑ_{\max}) using a quasi-Newton algorithm, giving a new vector of flowering parameters (β_{\max}). These parameters were then used to generate a new resident time-series and a second search was performed to determine the new β_{\max} . This process was repeated until successive values of ϑ_{\max} converged on 0 to a specified tolerance (0.001). The last β_{\max} was taken to be the putative ESS. To improve the precision of the estimate, a random-walk algorithm was used to find 250 strategies with fitness equal to the putative ESS (i.e. $\vartheta = 0$). This is necessary because when estimating ϑ to a finite level of precision a range of parameter values around the ESS have equal fitness. For each parameter of the flowering function, the mean of the resultant set of equal-fitness values was used as the final ESS estimate.

3. RESULTS**(a) Descriptive properties of the model**

The descriptive properties of the parameterized stochastic model can be assessed by calculating the stable size-age distribution numerically and comparing this with the observed data. This shows that there is good agreement between the model and the observed size-age distribution (figure 1). We also calculated various measures of population size and age structure, using the methods outlined in Rees & Rose (2002) and Childs *et al.* (2003), and in all cases the model predictions were in excellent agreement with the field data (table 1). As density dependence is explicitly modelled, we can calculate the equilibrium population size, and again there is excellent agreement between the model and the data (table 1).

(b) Fluctuating selection

Recently developed methods for analysing constant-environment integral projection models can be used to quantify the fluctuating selection pressure acting on the observed flowering strategy (Rees & Rose 2002; Childs *et al.* 2003). We take each year type in turn and assume that it describes a constant environment inhabited by a population employing the estimated flowering strategy. Two metrics summarizing the selection acting on the flowering strategy were then calculated for all 16 years: the ESS mean flowering size and the selection pressure on the intercept of the flowering function (β_0) (figure 2). The calculations were carried out assuming that the size-dependent slope of the flowering function, β_s , was fixed at the estimated value. We use this constraint to prevent the ESS strategy being a step function, which occurs as $\beta_s \rightarrow \infty$ and $\beta_a = 0$. The biological motivation for using this constraint is discussed in § 3c.

The ESS flowering strategy for each year type was determined by maximizing R_0 . The year-specific ESS flowering strategies were highly variable and fall into two broad categories, annual (mean flowering size of less than 30 mm) and delayed reproduction (mean flowering size of greater than 45 mm) types (figure 2a). The mean flowering size is approximately proportional to $-\beta_0$ and so sensitivities ($\partial \lambda / \partial \beta_0$) provide an estimate of the selection acting on the average size at flowering. In half the years, there is relatively weak selection for larger flowering sizes ($\partial \lambda / \partial \beta_0 < 0$), whereas in the remaining years there is much stronger selection for smaller flowering sizes ($\partial \lambda / \partial \beta_0 \gg 0$).

(c) Evolution of the flowering strategy

We initially calculated the ESS flowering strategy by allowing all three parameters of the flowering function to vary. Under these conditions, we find that the ESS flowering strategy tends to a step function with a very small age component (table 2). The predicted average size at flowering in this case is greater than the observed value, while the variance in flowering sizes is much lower than in the observed data (figure 3). We recalculated the ESS flowering strategy assuming that the size-dependent slope of the flowering function, β_s , is fixed at the estimated value, to prevent the flowering surface becoming a step function. There are several reasons why it might be impossible for plants to achieve a step function: (i) there is variable

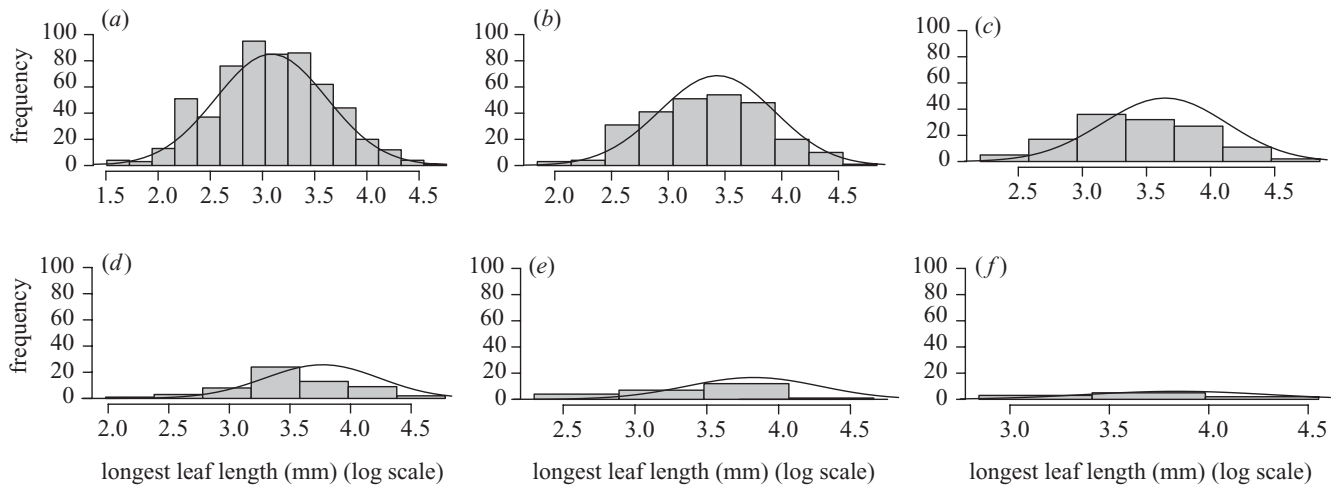


Figure 1. Observed (solid bars) and predicted (lines) stable size-age distribution for ages 0–5, in (a)–(f), respectively. The bar width in each histogram was chosen using a kernel density estimation routine to make the plots maximally informative.

Table 1. Field data and model predictions. (Values in brackets are 95% confidence intervals.)

	data	model
average number of plants	74.4 (47.9, 101)	78.2
average size (mm)	32.8 (31.5, 34.1)	32.9
average age (years)	0.84–0.94	0.96
average size at flowering (mm)	52.0 (48.4, 55.6)	55.1
average age at flowering (years)	3.1 (2.7, 3.4)	2.94

growth between when the decision to flower is made and when plant size is measured; (ii) plant size may not be perfectly correlated with the threshold condition for flowering; and (iii) there may be genetic variation in the threshold condition for flowering. When β_s is constrained, both the mean and variance of the predicted flowering-size distribution are in excellent agreement with the observed data (table 2; figure 3). There is effectively no age component to the ESS flowering function, which is intuitively sensible given that the vital rates are independent of age.

(d) *Fitness landscapes*

We generated a fitness landscape in the fully stochastic environment assuming that the resident used the estimated flowering strategy (figure 4). Fitness was calculated for a wide range of β_0 and β_a , assuming β_s was fixed. The ESS strategy lies just outside the 95% confidence envelope for the estimated parameters. Recall that as β_0 gets smaller (more negative) so the size at flowering increases. Moving across the landscape from left to right we see a steep increase in the performance of the flowering strategy, which reaches a maximum then declines to a plateau where all strategies have equal fitness. Clearly, flowering at sizes much larger than the ESS results in a dramatic loss of fitness. This is a consequence of high mortality: average-sized plants (32.8 mm) suffer between 15% and 95% mortality, depending on the year type. The plateau in the fitness landscape, corresponding to large values of β_0 , occurs as all plants adopt the annual flowering strategy, and so have equal performance. Moving vertically across the landscape, we see much smaller changes in

performance. This is a direct result of the vital rates being determined by plant size rather than by age.

The pattern of fluctuating selection (figure 2b) can be understood by examining the fitness landscape (figure 4). We assume that the general topography of the landscape is maintained in different years, though the location of the peak (i.e. the approximate ESS) may vary. In some years, the estimated strategy lies to the right of the peak on the plateau of early-flowering strategies, where there is only weak selection for flowering at larger sizes. In other years, the estimated strategy lies to the left of the ESS on the steep slope of strategies that delay flowering too long. In these instances, there is much stronger selection for flowering at smaller sizes.

To understand how different sources of variation influence the topography of the fitness surface, we calculated fitness landscapes in constant and stochastic environments. The geometry of a landscape depends in part upon the resident parameter set and not just on the underlying model. To illustrate this, we generated landscapes for five different resident populations in the stochastic environment, varying the parameter β_0 while fixing β_s and β_a at their estimated values (figure 5a). As the resident population moves further away from the ESS the shape and height of the fitness surface are altered. To control for this ‘resident location effect’, we used the environment-specific ESS parameters as the resident parameters when generating landscapes with different sources of temporal variation. Fitness landscapes were generated under five different regimes: a constant environment (using the average number of recruits and the average intercepts in the survival and growth models; justification for the use of this model is provided in Rees *et al.* (2004)), variable recruitment, variable survival, variable growth and the fully stochastic case. The ESS flowering strategy was estimated by varying only the parameter β_0 . Though the landscapes have the same general topography, the surface corresponding to the fully stochastic model has the sharpest peak (figure 5b). The largest differences between the landscapes occur at small flowering sizes ($-5 < \beta_0 < 0$). In this region, the net effect of stochastic growth is negligible relative to the constant-environment case. The relative fitness costs associated with early flowering in a variable-

Table 2. Evolutionarily stable flowering strategy in terms of the parameters of the flowering function and the average size and age at flowering, assuming that the slope of the flowering function, β_s , is constrained at its estimated value and no constraints. (For reference, the estimated values are also given, values in brackets are 95% confidence intervals.)

	parameter			mean	
	β_0	β_s	β_a	size at flowering (mm)	age at flowering (years)
unconstrained ESS	-507	131	-3.50	65.0	2.7
constrained ESS	-10.9	—	0.08	51.2	2.5
estimated value	-12.1 (-9.84, -14.26)	2.64 (2.06, 3.22)	0.32 (0.18, 0.45)	52.0 (48.4, 55.6)	2.8 (2.7, 3.4)

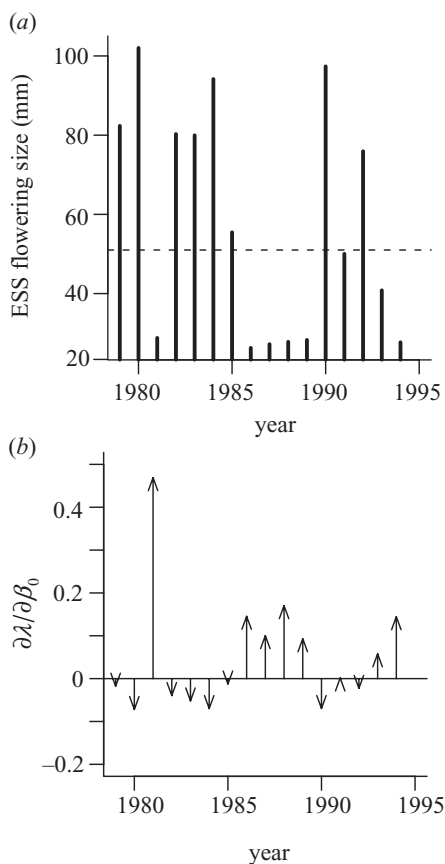


Figure 2. Demonstration of fluctuating selection in *Carlina* using (a) ESS flowering size for each year in a constant environment, the dashed line is the observed mean, and (b) selection pressure acting on the intercept of the flowering function, β_0 , in each year.

recruitment environment are much higher, lending support to the idea of a bet-hedging strategy operating in the system. By contrast, early flowering is less costly when survival is variable, because early reproduction reduces the impact of occasional high-mortality years. For large flowering sizes ($\beta_0 < -10$) the effects of stochastic variation are largely determined by variable survival, as indicated by the close approximation of the variable-survival-only model to the fully stochastic case.

(e) *Elasticity and sensitivity analysis*

The standard approach for understanding how the various parameters influence fitness is elasticities analysis. Elasticities can be used to measure the proportional

change in λ_s (not the invasion exponent = $\log \lambda_s$) caused by proportional changes in $f_a^{(i)}(x,y)$ and $p_a^{(i)}(x,y)$. Tuljapurkar (1990) presented a numerical method for estimating the elasticity of λ_s that is suitable for matrix models. We use this approach to generate an approximation for the elasticity of λ_s to the kernel component functions $k_{mn}(y_i, y_j)$, such that

$$\frac{\partial \log \lambda_s}{\partial \log k_{mn}(y_i, y_j)} = \lim_{T \rightarrow \infty} \frac{1}{T} \sum_{t=0}^{T-1} \frac{(\mathbf{v}(t+1) \mathbf{w}^T(t)) \circ \tilde{\mathbf{K}}^{(t)} \mathbf{D}}{R_t \mathbf{v}(t+1) \mathbf{w}^T(t+1)}, \quad (3.1)$$

where the m and n subscripts refer to the kernel component function in the m th row and n th column of $\tilde{\mathbf{K}}^{(t)}$, and \circ denotes the Hadamard operator. The terms $\mathbf{w}(t)$ and $\mathbf{v}(t)$ satisfy

$$\mathbf{w}(t+1) = \frac{\tilde{\mathbf{K}}^{(t)} \mathbf{D} \mathbf{w}(t)}{R_t} \quad \text{and} \quad \mathbf{v}^T(t-1) = \frac{\mathbf{v}^T(t) \tilde{\mathbf{K}}^{(t-1)} \mathbf{D}}{Q_t}, \quad (3.2)$$

where $R_t = \|\tilde{\mathbf{K}}^{(t)} \mathbf{w}(t) \mathbf{D}\|$ and $Q_t = \|\mathbf{v}^T(t) \tilde{\mathbf{K}}^{(t-1)} \mathbf{D}\|$ (see Caswell 2001, p. 402). Justification for the use of this approach is given in Appendix A. As elasticities sum to unity, this analysis allows us to partition the contributions of $f_a^{(i)}(x,y)$ and $p_a^{(i)}(x,y)$ to λ_s of different age classes. We also calculated elasticities for a constant-environment model (using the average number of recruits and the average intercepts in the survival and growth models). The elasticity surfaces corresponding to the constant and stochastic environments are almost identical (figure 6). They show that the survival-growth function makes a larger contribution to λ_s than does the fecundity function (constant environment, 0.70 and 0.30, respectively; stochastic environment, 0.67 and 0.33, respectively) and that the largest contributions to λ_s come from changes in the survival-growth function, $p_a^{(i)}(x,y)$, of young plants.

4. DISCUSSION

We have shown how the integral projection model may be used to explore the demography and evolution of size- and age-structured populations in a density-dependent stochastic environment. The resultant model combines the flexibility of the individual-based approach with the computational efficiency and power of traditional matrix methods. However, unlike parameterization of age- and size-structured matrix models (Law 1983), parameterization of the integral projection model is straightforward and requires no new techniques beyond standard regression analyses (Venables & Ripley 1997). Using

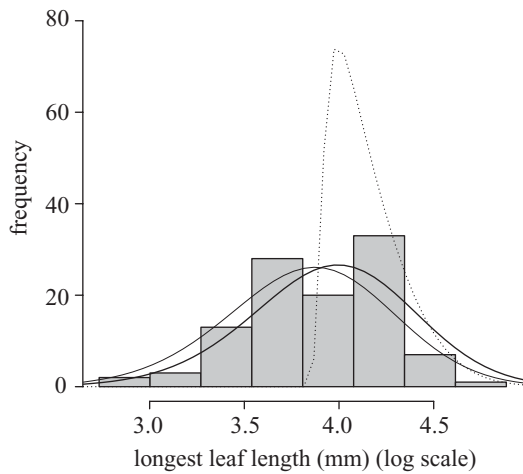


Figure 3. Observed distribution of flowering sizes (solid bars) and predictions from the various models. The bold line is the fitted model, the dotted line is from the unconstrained ESS model and the solid thin line is from the constrained ESS.

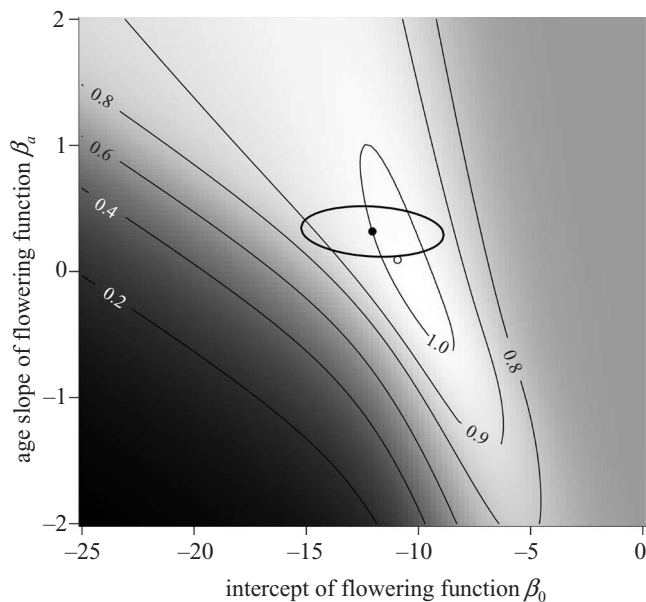


Figure 4. The fitness landscape for *Carlina*, calculated assuming that the resident population uses the estimated flowering strategy in a fully stochastic environment. The filled point is the estimated flowering strategy, and the bold ellipse is the 95% confidence contour, calculated using the standard quadratic approximation to the likelihood—assuming that the likelihood is χ^2 -distributed with three degrees of freedom. The open point is the ESS prediction assuming β_a is fixed.

simple field data, we were able to make very accurate predictions of the distribution of flowering sizes in *Carlina*. Invasibility analysis reveals that the observed flowering strategy is close to the ESS and that temporal variation in recruitment, growth and survival are all important influences on the evolutionarily stable flowering size (figure 5). These results reinforce the conclusions of Rees *et al.* (1999) and Rose *et al.* (2002) on the need to include temporal variation in life-history studies.

The parameterized model provides an accurate description of the number of individuals and the distribution of

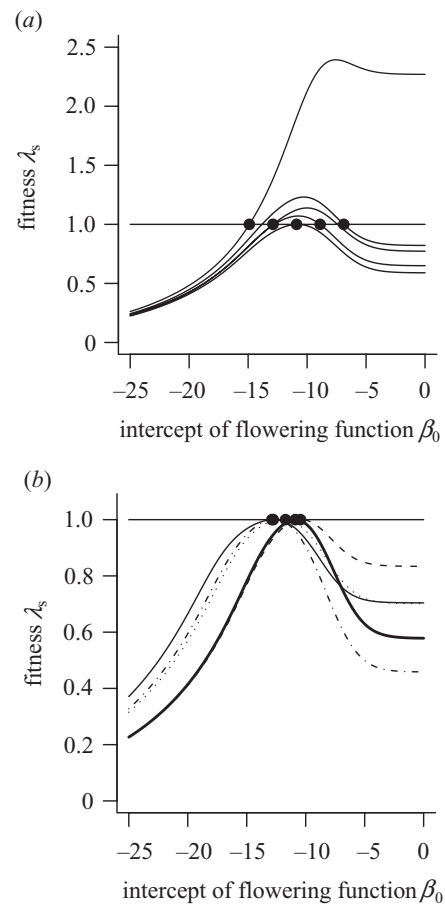


Figure 5. Fitness landscapes as a function of β_0 , the intercept of the flowering function: (a) stochastic environment with five different residents, (b) different variable environments with the environment-specific ESS as the resident strategy (thick line, fully stochastic environment; thin line, constant environment; dotted line, variable growth only; dashed line, variable survival only; dotted-dashed line, variable recruitment only).

sizes within each age class, the distribution of flowering sizes, average age at reproduction and average population size. Clearly, an adequate model must at least describe the data well if it is to be used to draw further conclusions. However, a parameterized model of *Carlina* ignoring stochastic variation failed to predict the mean and variance of the ESS flowering distribution, while still providing an accurate description of the population structure (Childs *et al.* 2003). By contrast, the stochastic model presented here predicts an evolutionarily stable flowering size (51.2 mm) that is very close to the estimated mean size at flowering (52.0 mm), provided that the variance in the threshold size distribution is constrained. Interestingly, in the constant-environment case (Childs *et al.* 2003), the parameters of the constrained ESS are not significantly different from the estimated parameters of the flowering function, yet the fitness difference between the estimated and evolutionarily stable flowering functions was *ca.* 10%. Conversely, in the stochastic model the ESS parameters are significantly different from the estimated parameters, though the fitness difference is only *ca.* 2%. Taken together, these observations indicate that an adequate description of the life history of *Carlina* needs to include temporal variation (Rose *et al.* 2002), and highlights the

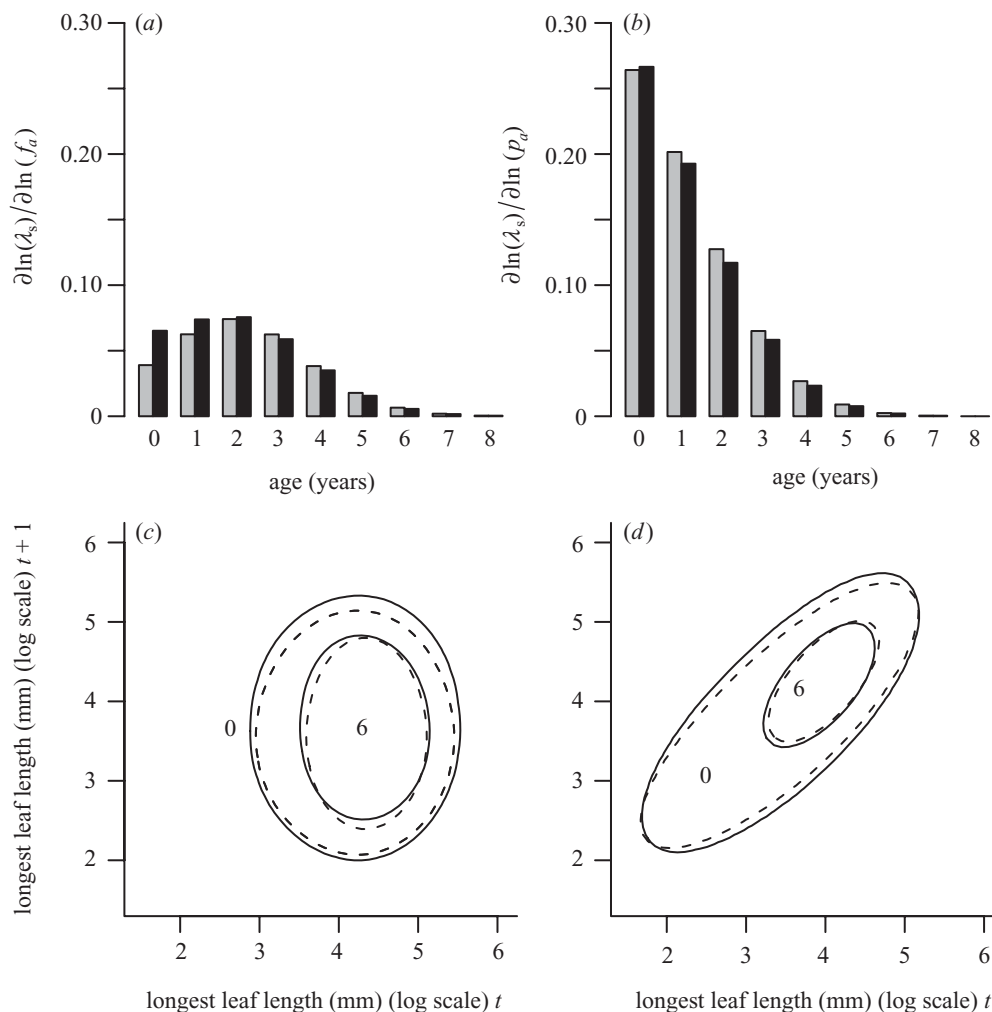


Figure 6. Elasticity analysis of the kernel component functions in constant (grey bars, dashed lines) and stochastic (black bars, continuous lines) models. Elasticity values summed over size for (a) $f_a(x,y)$ and (b) $p_a(x,y)$ for all ages. Elasticity contour plots for (c) $f_a(x,y)$ and (d) $p_a(x,y)$ for ages 0 and 6, showing the 0.000 003 contour for each age.

need to be careful when comparing the predictions of evolutionary models with data, as different metrics may produce different results. It is also important to distinguish between biological significance (measured in terms of fitness differences) and statistical significance when making such comparisons.

The fitness landscapes (figure 5b) have well-defined maxima in contrast to those of several other studies (Klinkhamer & de Jong 1983; Tuljapurkar 1990), and the sharpness of the peak increases as different forms of stochasticity are included in the model (figure 5). This discrepancy between our study and earlier studies is probably a result of exploring models with several forms of stochasticity. The importance of different sources of stochasticity depends on flowering size; in large flowering plants, fitness is primarily determined by fluctuations in survival, whereas in small flowering ones fluctuations in recruitment are critical. Thus, the generalization of Caswell (2001), that in stochastic environments fitness optima are often flat, may be a consequence of including only a single form of stochasticity in earlier models.

Selection and common garden experiments have shown that natural populations harbour extensive genetic variation for flowering size (reviewed in Metcalf *et al.* 2003). The mechanisms responsible for the maintenance

of this variation are not known but theoretical work has shown that an evolutionarily stable population has a positive genetic variance maintained by selection providing that the product of the variance of fluctuations, the amount of generation overlap and the selection intensity is sufficiently high (Ellner & Hairston 1994). This mechanism could operate in *Carlina* as there is fluctuating selection (figure 2b) and overlapping generations.

Elasticity analysis was used to partition contributions to λ_s from different kernel component functions, age classes and sizes. In this system the survival-growth functions make a greater contribution to λ_s than the fecundity functions, because reductions in growth and survival of a particular age class reduce opportunities for reproduction in subsequent years. Younger plants contribute most to λ_s because they represent a larger proportion of the stable age distribution. However, this underlying trend is tempered by the fact that younger, and hence smaller, plants contribute relatively few recruits to the next generation (figure 6a,b). Elasticity contour plots for the fecundity functions demonstrate that contributions to λ_s through recruitment are most important for large individuals, while λ_s is influenced by the survival of a wide range of size types (figure 6c,d). Individuals are, on average, larger as they grow older, and this is reflected in a shift in the

high-density regions of the elasticity surfaces toward larger sizes for older age classes. As found in several other studies, the constant-environment elasticities provide an excellent approximation to the stochastic-environment ones (Benton & Grant 1996; Caswell 2001).

By combining techniques for the modelling of size- and age-dependent demography in a stochastic environment with ideas from evolutionary demography we have been able to show that the observed flowering strategy in *Carlina* is close to the ESS and that accurate prediction of the distribution of flowering sizes is possible. What is not clear is how different forms of stochasticity influence the ESS. There are two distinct ways in which temporal variation could be important. First, when the environment varies through time, average demographic rates differ from demographic rates in the average environment owing to nonlinear averaging. Second, the ESS will vary from year to year, owing to non-equilibrium dynamics. Methods for quantifying the relative importance of different forms of stochasticity and how nonlinear averaging and non-equilibrium dynamics contribute to this are explored in Rees *et al.* (2004) where techniques for decomposing the effects of stochastic selection are developed.

APPENDIX A: STOCHASTIC GROWTH RATE AND SENSITIVITY ANALYSIS

We supply some technical details for the *C. vulgaris* model; more general models will be considered elsewhere. As in the corresponding deterministic model (appendix to Childs *et al.* 2003), some special model properties allow derivations based on matrix-model theory:

- (i) all living individuals have some probability of reproducing now or later;
- (ii) there is a maximum possible age, m ; and
- (iii) the size distribution of new offspring (age = 0) is the same for all parents in all years:

$$f_d(x, y) = \varphi_0(y), \tag{A 1}$$

with the environment states $\tau(t)$ determining the survival and growth functions and the total number of recruits each year.

As a result of (ii) and (iii), after an initial transient of, at most, m years the state of living individuals is a function only of the environment states ‘now’ and over the past m years, $\theta(t) = (\tau(t), \tau(t - 1), \dots, \tau(t - m))$. Consider individuals now of some age a .

- (i) One component of $\theta(t)$ determines the number of recruits R_{t-a} in their year of birth, and thus determines the initial cohort as $n_0(x, t - a) = R_{t-a}\varphi_0(x)$.
- (ii) Other components of $\theta(t)$ then determine the survival and growth functions that act on this cohort in each subsequent year up to the present.

Thus, the entire resident population state at time t is a deterministic function of the random environment process $\theta(t)$.

By assumption, the environment states $\tau(t)$ are independent and identically distributed, hence $\theta(t)$ is a stationary ergodic first-order Markov chain. The resident-population process is therefore stationary and ergodic (with stochastic growth 0, neither increasing nor decreasing). Its numerical properties can be determined either by simulation and averaging, or by numerically

implementing the population-dynamic iterations (using the $\tau(t)$ -dependent kernel components) that generate the current population state as a function of $\theta(t)$.

An invader’s population dynamics are density independent with equations (2.9) and (2.15) giving the fecundity (survival and growth are density independent for both resident and invader). All terms in these equations are functions of $\theta(t)$, either directly or via the dependence of the resident-population state on $\theta(t)$. The invader is therefore governed by a stochastic density-independent integral projection model in which all components depend on $\theta(t)$. However, this can be reduced to a stochastic matrix model for the total number of individuals in each age class, implying the existence of a stochastic growth rate, as follows.

As with the resident, after a possible transient of length m all individuals of ages $j > 0$ are descended from a cohort with size distribution φ_0 and therefore have size distributions proportional to $\varphi_j(y, t)$ where

$$\begin{aligned} \psi_{j+1}(y, t + 1) &= \int_{\Omega} \varphi_j(x, t) p_j^{(j)}(x, y) dx, \\ \varphi_{j+1} &= \psi_{j+1} / \int_{\Omega} \psi_{j+1} dy. \end{aligned} \tag{A 2}$$

The fraction surviving to age $j + 1$ is therefore

$$P_j(t) = \iint_{\Omega} \varphi_j(x, t) p_j^{(j)}(x, y) dx dy. \tag{A 3}$$

Note that, since φ_0 is independent of time, equation (A 2) constructs $\varphi_j(y, t)$ as a function of $\theta(t)$, hence $P_j(t)$ is a function of $\theta(t)$. Similarly, the *per capita* fecundity of age- j individuals is

$$F_j(t) = \iint_{\Omega} \varphi_j(x, t) f_j^{(j)}(x, y) dx dy. \tag{A 4}$$

As noted above, $f_j^{(j)}$ is determined by $\theta(t)$, so $F_j(t)$ is also determined by $\theta(t)$. The population count vector $\mathbf{N}(t) = [N_0(t), N_1(t), \dots, N_m(t)]$, consisting of the total numbers in each age class, therefore satisfies a stochastic Leslie matrix $\mathbf{L}^{(t)}$ having the same form as the $\tilde{\mathbf{K}}^{(t)}\mathbf{D}$ matrix (equations (2.6) and (2.7)),

$$\mathbf{N}(t + 1) = \begin{pmatrix} F_0(t) & F_1(t) & \dots & F_{m-1}(t) & F_m(t) \\ P_0(t) & 0 & \dots & 0 & 0 \\ \vdots & P_1(t) & & \vdots & \vdots \\ & \vdots & \ddots & & \\ 0 & 0 & \dots & P_{m-1}(t) & 0 \end{pmatrix} \mathbf{N}(t). \tag{A 5}$$

The random matrix sequence $\mathbf{L}^{(t)}$ is stationary and ergodic, and its values lie in an ergodic set (there are 16^{m+1} possible values of $\theta(t)$ each generating a possible value of $\mathbf{L}^{(t)}$, and all have the same incidence matrix which is power-positive). The fact that the set of values of $\mathbf{L}^{(t)}$ is finite also implies that $E \max\{0, \log \|\mathbf{L}^{(t)}\|\}$ is finite, hence standard results for stochastic matrix models (see Tuljapurkar (1990), § 4.2.1) imply the existence of a unique stochastic growth rate, which is independent of the initial population vector.

The elasticity analysis (equations (3.1) and (3.2)) depends on two additional properties (see Tuljapurkar (1990), § 11.2). First, the process $\theta(t)$ generating the vital rates can be run backwards in time by running $\tau(t)$ backwards in time, which is possible since values of $\tau(t)$ are generated independently over time. Second, the reduction to a matrix model above implies that the growth rate is a smooth function under perturbations of the matrix (and hence under perturbations of the integral model kernel components that generate the matrix). Equations (3.1) and (3.2) therefore give the elasticity of the *approximate* stochastic growth rate generated by the quadrature approximation to the stochastic integral model (i.e. the $\tilde{\mathbf{K}}^{(Q)}\mathbf{D}$ matrix). In other words, by formally reducing the model to equation (A 5) we have shown that the stochastic growth rate exists and has well-defined elasticities. The calculations in § 3e involving the $\tilde{\mathbf{K}}^{(Q)}\mathbf{D}$ matrix are a straightforward way to obtain approximate numerical values of these quantities (to any desired accuracy, by increasing the number of mesh points) using standard matrix operations and software.

REFERENCES

- Benton, T. G. & Grant, A. 1996 How to keep fit in the real-world: elasticity analyses and selection pressures on life-histories in a variable environment. *Am. Nat.* **147**, 115–139.
- Caswell, H. 2001 *Matrix population models. Construction, analysis and interpretation*. Sunderland, MA: Sinauer Associates.
- Charlesworth, B. 1994 *Evolution in age-structured populations*. Cambridge Studies in Mathematical Biology. Cambridge University Press.
- Childs, D. Z., Rees, M., Rose, K. E., Grubb, P. J. & Ellner, S. P. 2003 Evolution of complex flowering strategies: an age- and size-structured integral projection model approach. *Proc. R. Soc. Lond. B* **270**, 1829–1838. (DOI 10.1098/rspb.2003.2399.)
- Cole, L. C. 1954 The population consequences of life history phenomena. *Q. Rev. Biol.* **29**, 103–137.
- de Jong, T. J., Klinkhamer, P. G. L., Geritz, S. A. H. & van der Meijden, E. 1989 Why biennials delay flowering—an optimization model and field data on *Cirsium vulgare* and *Cynoglossum officinale*. *Acta Bot. Neerland.* **38**, 41–55.
- de Jong, T. J., Klinkhamer, P. G. L. & de Heiden, J. L. H. 2000 The evolution of generation time in metapopulations of monocarpic perennial plants: some theoretical considerations and the example of the rare thistle *Carlina vulgaris*. *Evol. Ecol.* **14**, 213–231.
- Easterling, M. R. 1998 The integral projection model: theory, analysis and application. PhD thesis, North Carolina State University, Raleigh, NC, USA.
- Easterling, M. R., Ellner, S. P. & Dixon, P. M. 2000 Size-specific sensitivity: applying a new structured population model. *Ecology* **81**, 694–708.
- Ellner, S. & Hairston, N. G. 1994 Role of overlapping generations in maintaining genetic variation in a fluctuating environment. *Am. Nat.* **143**, 403–417.
- Eriksson, A. & Eriksson, O. 1997 Seedling recruitment in semi-natural pastures: the effects of disturbance, seed size, phenology and seed bank. *Nordic J. Bot.* **17**, 469–482.
- Kachi, N. & Hirose, T. 1985 Population dynamics of *Oenothera glazioviana* in a sand-dune system with special reference to the adaptive significance of size-dependent reproduction. *J. Ecol.* **73**, 887–901.
- Klinkhamer, P. G. L. & de Jong, T. J. 1983 Is it profitable for biennials to live longer than two years? *Ecol. Model.* **20**, 223–232.
- Klinkhamer, P. G. L., de Jong, T. J. & Meelis, E. 1987 Delay of flowering in the biennial *Cirsium vulgare*: size effects and devernalization. *Oikos* **49**, 303–308.
- Klinkhamer, P. G. L., de Jong, T. J. & Meelis, E. 1991 The control of flowering in the monocarpic perennial *Carlina vulgaris*. *Oikos* **61**, 88–95.
- Klinkhamer, P. G. L., de Jong, T. J. & de Heiden, J. L. H. 1996 An eight-year study of population dynamics and life-history variation of the ‘biennial’ *Carlina vulgaris*. *Oikos* **75**, 259–268.
- Law, R. 1983 A model for the dynamics of a plant population containing individuals classified by age and size. *Ecology* **64**, 224–230.
- Metcalfe, J. C., Rose, K. E. & Rees, M. 2003 Evolutionary demography of monocarpic perennials. *Trends Ecol. Evol.* **18**, 471–480.
- Metz, J. A. J., Nisbet, R. M. & Geritz, S. A. H. 1992 How should we define ‘fitness’ for general ecological scenarios? *Trends Ecol. Evol.* **7**, 198–202.
- Mylius, S. D. & Diekmann, O. 1995 On evolutionarily stable life histories, optimization and the need to be specific about density dependence. *Oikos* **74**, 218–224.
- Rees, H., Childs, D. Z., Rose, K. E. & Grubb, P. J. 2004 Evolution of size-dependent flowering in a variable environment: partitioning the effects of fluctuating selection. *Proc. R. Soc. Lond. B* **271**. (In the press.) (DOI 10.1098/rspb.2003.2596.)
- Rees, M. & Rose, K. E. 2002 Evolution of flowering strategies in *Oenothera glazioviana*: an integral projection model approach. *Proc. R. Soc. Lond. B* **269**, 1509–1515. (DOI 10.1098/rspb.2002.2037.)
- Rees, M., Sheppard, A., Briese, D. & Mangel, M. 1999 Evolution of size-dependent flowering in *Onopordum illyricum*: a quantitative assessment of the role of stochastic selection pressures. *Am. Nat.* **154**, 628–651.
- Rees, M., Mangel, M., Turnbull, L. A., Sheppard, A. & Briese, D. 2000 The effects of heterogeneity on dispersal and colonisation in plants. In *Ecological consequences of environmental heterogeneity* (ed. M. J. Hutchings, E. A. John & A. J. A. Stewart), pp. 237–265. Oxford: Blackwell Scientific.
- Rees, H., Childs, D. Z., Rose, K. E. & Grubb, P. J. 2004 Evolution of size-dependent flowering in a variable environment: partitioning the effects of fluctuating selection. *Proc. R. Soc. Lond. B* **271**. (In the press.) (DOI 10.1098/rspb.2003.2596.)
- Roff, D. A. 1992 *The evolution of life histories. Theory and analysis*. London: Chapman & Hall.
- Rose, K. E., Rees, M. & Grubb, P. J. 2002 Evolution in the real world: stochastic variation and the determinants of fitness in *Carlina vulgaris*. *Evolution* **56**, 1416–1430.
- Sletvold, N. 2002 Effects of plant size on reproductive output and offspring performance in the facultative biennial *Digitalis purpurea*. *J. Ecol.* **90**, 958–966.
- Stearns, S. C. 1992 *The evolution of life histories*. Oxford University Press.
- Tuljapurkar, S. 1990 *Population dynamics in variable environments*. Lecture Notes in Biomathematics. London: Springer.
- Venables, W. N. & Ripley, B. D. 1997 *Modern applied statistics with S-PLUS*. New York: Springer.
- Weiner, J., Martinez, S., Muller-Scharer, H., Stoll, P. & Schmid, B. 1997 How important are environmental maternal effects in plants? A study with *Centaurea maculosa*. *J. Ecol.* **85**, 133–142.
- Wesselingh, R. A., Klinkhamer, P. G. L., de Jong, T. J. & Boorman, L. A. 1997 Threshold size for flowering in different habitats: effects of size-dependent growth and survival. *Ecology* **78**, 2118–2132.

As this paper exceeds the maximum length normally permitted, the authors have agreed to contribute to production costs.